Cell, Vol. 97, 515–525, May 14, 1999, Copyright ©1999 by Cell Press

Short Dysfunctional Telomeres Impair Tumorigenesis in the INK4a$^{\Delta 2/3}$ Cancer-Prone Mouse

Roger A. Greenberg,[4] Lynda Chin,[1,3] Andrea Femino,[5] Kee-Ho Lee,[1] Geoffrey J. Gottlieb,[6] Robert H. Singer,[5] Carol W. Greider,[7] and Ronald A. DePinho[1,2,8]

[1]Department of Adult Oncology
Dana-Farber Cancer Institute
44 Binney Street
Boston, Massachusetts 02115
[2]Department of Medicine and Genetics
[3]Department of Dermatology
Harvard Medical School
Boston, Massachusetts 02115
[4]Department of Microbiology and Immunology
[5]Department of Structural Biology and Anatomy
Albert Einstein College of Medicine
Bronx, New York 10461
[6]Quest Diagnostics Inc.
Anatomic Pathology
Teterboro, New Jersey 07608
[7]Department of Molecular Biology and Genetics
Johns Hopkins University School of Medicine
Baltimore, Maryland 21205

Summary

Maintenance of telomere length is predicted to be essential for bypass of senescence and crisis checkpoints in cancer cells. The impact of telomere dysfunction on tumorigenesis was assessed in successive generations of mice doubly null for the telomerase RNA (*mTR*) and the *INK4a* tumor suppressor genes. Significant reductions in tumor formation in vivo and oncogenic potential in vitro were observed in late generations of telomerase deficiency, coincident with severe telomere shortening and associated dysfunction. Reintroduction of *mTR* into cells significantly restored the oncogenic potential, indicating telomerase activation is a cooperating event in the malignant transformation of cells containing critically short telomeres. The results described here demonstrate that loss of telomere function in a cancer-prone mouse model possessing intact DNA damage responses impairs, but does not prevent, tumor formation.

Introduction

The finite replicative capacity of primary human cells, or Hayflick limit (Hayflick and Moorehead, 1961), has been proposed as a tumor suppression mechanism in vivo (Dykhuizen, 1974 and reviewed in Sager, 1991). One of the cellular events that signals entry into replicative senescence is telomere shortening (Harley et al., 1990; Bodnar et al., 1998; Vaziri and Benchimol, 1998). Viral oncoprotein-induced inactivation of pRB and p53 allows for extended cell division beyond the Hayflick limit (also known as mortality stage 1 [M1]), suggesting that these tumor suppressor pathways are critical mediators of this telomere length checkpoint response (reviewed in Wright and Shay, 1995). Cellular proliferation beyond M1 is associated with significant telomere shortening and eventually a second block to continued proliferation, termed "crisis" (or mortality stage 2 [M2]). Crisis is a period in which cultured cells experience extreme genomic instability and massive cell death (Hara et al., 1991; Shay et al., 1991).

Thus, it appears that would-be cancer cells must negotiate two prominent telomere-based tumor suppression mechanisms, replicative senescence and crisis. Indeed, the rare immortalized clones that emerge from crisis restore their telomere function, most commonly through activation of the telomerase holoenzyme. Less often, telomere restoration in postcrisis human cells can be achieved through a telomerase-independent alternative telomere maintenance mechanism, referred to as ALT. ALT cells have long heterogeneous telomeres thought to be generated by a recombination-based mechanism (Bryan et al., 1995, 1997). In yeast, telomerase-independent telomere elongation occurs via a gene conversion pathway. In telomerase-deficient strains, a *RAD52*-dependent recombination mechanism restores telomere length in *S. cerevisiae* and *K. lactis* (Lundblad and Blackburn, 1993; McEachern and Blackburn, 1996), while *S. pombe* stabilizes its genome through chromosomal circularization (Naito et al., 1998; Nakamura et al., 1998) or telomere lengthening via a mechanism that may also represent a recombination-based process (Naito et al., 1998; Nakamura et al., 1998).

Reports that ectopic expression of telomerase activity alone (Bodnar et al., 1998; Vaziri and Benchimol, 1998), or together with compromise of the Rb pathway (Kiyono et al., 1998), can significantly extend cellular replicative capacity of primary human cells firmly establish a role for telomere shortening as a signal for M1 checkpoint activation. Additional evidence, however, indicates that other interventions exist that can also activate the senescence program independent of telomere shortening (Serrano et al., 1996; Lloyd et al., 1997; Lin et al., 1998; Zhu et al., 1998). More recent evidence has demonstrated that telomere maintenance by telomerase can prevent crisis in postsenescent SV40 large T antigen (T-Ag) transformed human embryonic kidney cells and lung fibroblasts containing a targeted deletion of the CDK inhibitor gene *p21$^{CIP1/WAF1}$* (Counter et al., 1998). Indeed, a critical role for telomere maintenance in evading M1 and M2 was suggested by the activation of telomerase (reviewed in Kim et al., 1994; Bacchetti, 1996) or ALT mechanism (Bryan et al., 1997) in nearly 100% of human immortalized cell lines or primary tumors, implying that telomere function is essential for the continued growth of immortal cells.

The behavior of rodent cells in culture differs from that of human cells in several respects. The laboratory mouse *Mus musculus* possesses very long telomeres while mouse embryonic fibroblasts (MEFs) undergo a block to cell division following only 10–20 population doublings (PDs) in culture. This block to cell growth

[8]To whom correspondence should be addressed (e-mail: ron_depinho@dfci.harvard.edu).

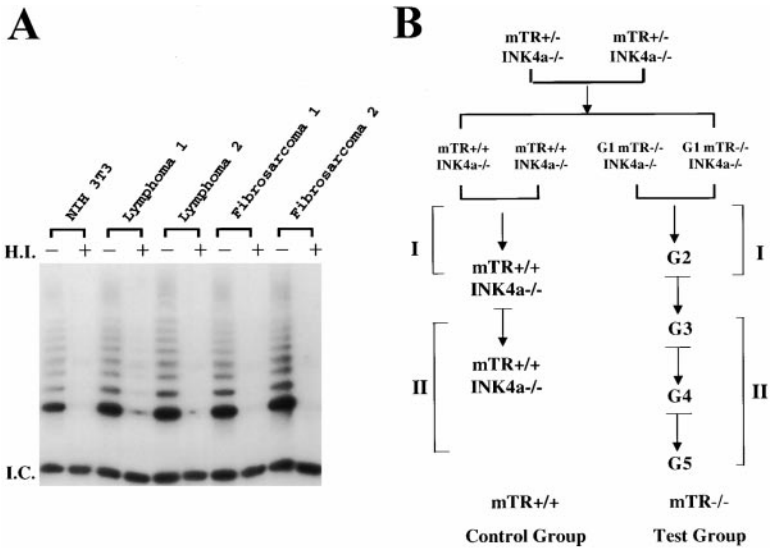

Figure 1. Telomerase Activity in $mTR^{+/+}$ $INK4a^{-/-}$ Tumors and Design of In Vivo Tumorigenesis Studies

(A) TRAP assay of telomerase activity in four independently derived $mTR^{+/+}$ $INK4a^{-/-}$ tumors. Assays were run on 1000 cells for each sample. NIH 3T3 cells were used as a positive control for mouse telomerase activity. Heat inactivation (H.I.) of samples was used as a negative control for activity as indicated in the figure. A PCR internal control (I.C.) was used as indicated to obtain a relative estimate of telomerase activity between samples.

(B) Mating scheme and design of in vivo tumorigenesis studies. Mating of $mTR^{+/-}$ $INK4a^{-/-}$ mice produced $mTR^{+/+}$ $INK4a^{-/-}$ and G1 $mTR^{-/-}$ $INK4a^{-/-}$ mice in the expected Mendelian ratio. G1 $mTR^{-/-}$ $INK4a^{-/-}$ mice were crossed to produce the second generation double null group, G2. Matings within the same generation of mTR deficiency produced the subsequent generation as indicated. I and II refer to the two separate groups of mice studied. G1 and G2 mice underwent carcinogenesis protocols at the same time in group I, while G3, G4, and G5 mice were studied together in group II. $mTR^{+/+}$ $INK4a^{-/-}$ mice were used as a positive control comparison during carcinogenesis studies for group I and group II.

has been referred to as senescence by analogy to the behavior of human cells. Although mouse and human cells share many morphological and biochemical features upon entry into senescence, the very long length of mouse telomeres makes it unlikely that telomere shortening provides a signal to activate the senescence program. In the absence of a telomere sensing mechanism, the question of why telomerase is consistently upregulated in immortalized and transformed mouse cultures could relate to less stringent control of mouse telomerase and *TERT* gene expression (Prowse and Greider, 1995; Greenberg et al., 1998; Martin-Rivera et al., 1998) and/or its regulation by proliferative factors such as the Myc oncoprotein (Wang et al., 1998; Greenberg et al., 1999; Wu et al., 1999). Moreover, telomerase activation in these settings does not appear to be essential, since telomerase-deficient (i.e., homozygous null for telomerase RNA, $mTR^{-/-}$) MEFs immortalize in culture and form tumors following viral oncogenesis in nude mice (Blasco et al., 1997). On the other hand, telomere maintenance in normal cells clearly plays a critical role in preserving the genomic stability and long-term viability of highly proliferative organ systems (Lee et al., 1998). Specifically, defects in germ cell growth and survival, uterine and intestinal atrophy, and impaired lymphocyte mitogenesis, hematopoiesis, and wound healing were evident in the later generations of *mTR* null mice (Lee et al., 1998; Rudolph et al., 1999). Reports of proliferative defects in *mTR* null ES cells after 300 population doublings and cessation of growth at approximately 450 population doublings also point to the necessity of maintaining telomeres via telomerase-dependent mechanisms in cultured mouse cells (Niida et al., 1998).

The compromise of proliferative organs in late-generation *mTR* null mice, and the evidence for possible requirement of telomerase in tumorigenesis, prompted us to evaluate the rate of tumor formation and cellular transformation in mice doubly null for *INK4a* ($INK4a^{-/-}$) and telomerase ($mTR^{-/-}$). The *INK4a/ARF* locus produces two distinct gene products, $p16^{INK4a}$ and $p19^{ARF}$, which are modulators of the pRB and p53 pathways, respectively (reviewed in Sherr, 1998). $p16^{INK4a}$ expression causes a G1 arrest by inhibiting cyclin-dependent kinases 4 and 6, thus preventing pRB hyperphosphorylation, and S phase entry (Serrano et al., 1993). $p19^{ARF}$ interacts with MDM2 and abrogates MDM2-induced degradation of p53 through the ubiquitin/proteosome pathway (Kamijo et al., 1998; Pomerantz et al., 1998; Stott et al., 1998; Zhang et al., 1998). While $p19^{ARF}$ has been shown to mediate p53-dependent apoptosis induced by oncogenic stimuli (de Stanchina et al., 1998; Palermo et al., 1998; Radfar et al., 1998; Zindy et al., 1998) and Rb deficiency (Bates et al., 1998; Pomerantz et al., 1998), it is not required for activation of the p53 checkpoint function in response to DNA damage (Kamijo et al., 1997; Stott et al., 1998).

For purposes of this study, several features of the $INK4a^{\Delta 2/3}$ model are worth noting, including its highly penetrant cancer phenotype and the facts that $INK4a^{-/-}$ MEFs are readily transformed by cellular oncogenes, exhibit a high rate of colony formation, and lack a senescent arrest phase in culture (Serrano et al., 1996). These findings have marked *INK4a/ARF* as a key tumor suppressor locus encoding essential mediators of cellular senescence. These experimental attributes, together with intact DNA damage responses (Kamijo et al., 1997), establish the $INK4a^{\Delta 2/3}$ mouse as an ideal in vivo system in which to assess the importance of telomere function in the tumorigenic process.

Results

Impact of Telomerase and Telomere Function on the $INK4a^{\Delta 2/3}$ Cancer Phenotype of Mice

Strong telomerase activation is correlated with tumorigenesis in several mouse models (Chadeneau et al., 1995; Bednarek et al., 1996; Blasco et al., 1996; Broccoli et al., 1996). To determine whether tumors derived from $INK4a^{-/-}$ null mice activate telomerase, the telomerase activity assay (TRAP) (Kim et al., 1994) was used in

A

Genotype	mTR+/+ INK4a-/-	mTR+/- INK4a-/-	G1 mTR-/- INK4a-/-	G2 mTR-/- INK4a-/-
# Mice Analyzed	14	16	13	19
Tumor Incidence (%)	6 (43%)	8 (50%)	7 (54%)	9 (47%)
Mean Latency (wks)	10	11	11	10

B

Genotype	mTR+/+ INK4a-/-	G3 mTR-/- INK4a-/-	G4 mTR-/- INK4a -/-	G5 mTR-/- INK4a-/-
# Mice Analyzed	25	12	16	26
Tumor Incidence (%)	16 (64%)	6 (50%)	5 (31%)	8 (31%)
Mean Latency (wks)	9.5	11	13	10
# Survived (%)	3 (12%)	4 (33%)	7 (44%)	14 (54%)

C

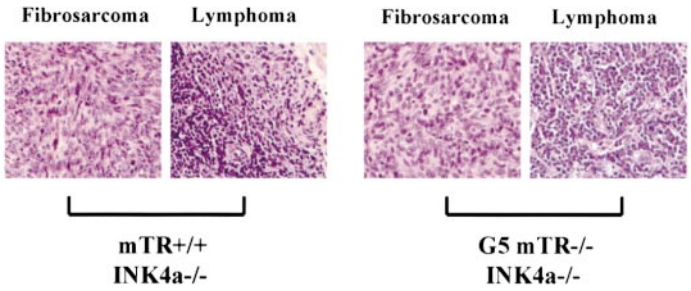

Figure 2. In Vivo Incidence of Tumor Formation and Survival in $mTR^{-/-}$ Mice

(A and B) Mice underwent two-step carcinogenesis protocols as described in Experimental Procedures. The number of mice analyzed for each genotype, tumor incidence and latency, and survival during the 16-week study is indicated.

(C) Representative histology of tumor samples for $mTR^{+/+}$ $INK4a^{-/-}$ and G5 $mTR^{-/-}$ $INK4a^{-/-}$ groups. Aggressive fibrosarcomas and B cell lymphomas are revealed for both groups by hematoxylin and eosin staining of paraffin-embedded sections.

$INK4a^{-/-}$ tumors arising spontaneously or induced after carcinogenesis. In all tumors tested (five fibrosarcomas and three B cell lymphomas), telomerase activity was detected at levels greater than those observed in nontransformed NIH 3T3 fibroblasts (for representative examples, see Figure 1A). The much lower levels in nontransformed mouse cells and consistent activation of telomerase in the eight $INK4a^{-/-}$ tumors support the use of this model to determine the role of telomerase and telomere function in the development of primary solid and lymphoid tumors.

Successive generations of mice doubly null for *mTR* and *INK4a* were mated to yield large cohorts of mice possessing progressively shorter telomeres (Blasco et al., 1997, and data not shown). Specifically, intercrosses between $mTR^{+/-}$ $INK4a^{-/-}$ mice produced the first generation of $mTR^{-/-}$ $INK4a^{-/-}$ mice (termed G1 $mTR^{-/-}$ $INK4a^{-/-}$). These G1 $mTR^{-/-}$ $INK4a^{-/-}$ mice were then intercrossed to produce second-generation $mTR^{-/-}$ $INK4a^{-/-}$ mice (termed G2 $mTR^{-/-}$ $INK4a^{-/-}$) and so on (Figure 1B). This mating strategy was pursued until the fifth generation, at which point diminished fecundity precluded the production of G6 $mTR^{-/-}$ $INK4a^{-/-}$ mice (Lee et al., 1998). As reported previously, $INK4a^{-/-}$ mice are highly cancer prone, exhibiting high rates of fibrosarcomas and B cell lymphomas following exposure to a two-step DMBA/UVB carcinogenesis protocol (Serrano et al., 1996; see Experimental Procedures). To compare more precisely the cancer incidence of $mTR^{+/+}$ $INK4a^{-/-}$ mice with that of the G1-G5 $mTR^{-/-}$ $INK4a^{-/-}$ mice, mice generated during the same period were monitored in parallel (Figure 1B). In the first study (Figure 2A), $mTR^{+/+}$ $INK4a^{-/-}$ mice were compared with G1 $mTR^{-/-}$ $INK4a^{-/-}$ and G2 $mTR^{-/-}$ $INK4a^{-/-}$ mice; while in the second phase (Figure 2B), another group of $mTR^{+/+}$ $INK4a^{-/-}$ mice was compared with G3 through G5 $mTR^{-/-}$ $INK4a^{-/-}$ mice.

In the first investigation, the incidence, latency, clinical behavior, and histological grade of primary tumors were remarkably similar among the $mTR^{+/+}$ $INK4a^{-/-}$ and G1-G2 $mTR^{-/-}$ $INK4a^{-/-}$ groups (Figure 2A). In the second set of experiments, a modest reduction in tumor incidence was first evident in the G3 $mTR^{-/-}$ $INK4a^{-/-}$ group and became more marked in the G4 and G5 $mTR^{-/-}$ $INK4a^{-/-}$ groups (Figure 2B). Specifically, tumors developed in 16 of 25 (64%) $mTR^{+/+}$ $INK4a^{-/-}$ mice, compared to 13 of 42 (31%) for the G4 and G5 $mTR^{-/-}$ $INK4a^{-/-}$ groups combined. Compared to the wild-type mTR cohort, the decrease in tumor formation was statistically significant for G4 $mTR^{-/-}$ $INK4a^{-/-}$ ($p = 0.0407$), G5 $mTR^{-/-}$ $INK4a^{-/-}$ ($p = 0.0175$), and G4 and G5 $mTR^{-/-}$ $INK4a^{-/-}$ combined ($p = 0.0083$). The distribution of tumor types was similar in all groups—11 fibrosarcomas and 5 B cell lymphomas confirmed in the $mTR^{+/+}$

INK4a$^{-/-}$ mice and 9 fibrosarcomas and 4 B cell lymphomas diagnosed in the G4-G5 *mTR*$^{-/-}$ *INK4a*$^{-/-}$ mice. Notably, despite a reduction in tumor incidence, the histological appearance (tumor grade and severity) of the 8 G4 and G5 *mTR*$^{-/-}$ *INK4a*$^{-/-}$ tumors analyzed was indistinguishable from that of the *mTR*$^{+/+}$ *INK4a*$^{-/-}$ tumors analyzed (Figure 2C). The reduction in tumor incidence in the later generations was also correlated with an increase in survival, although a definitive cause of death due to tumor burden was not always possible to establish in all cases. Correspondingly, while only 3 of 25 (12%) *mTR*$^{+/+}$ *INK4a*$^{-/-}$ mice were alive at the end of the experiment, 4 of 12 (33%) G3 *mTR*$^{-/-}$ *INK4a*$^{-/-}$; 7 of 16 (44%) G4 *mTR*$^{-/-}$ *INK4a*$^{-/-}$; and 14 of 26 (54%) G5 *mTR*$^{-/-}$ *INK4a*$^{-/-}$ mice survived. This increasing trend in survival was significant by the log rank test when comparing survival curves between *mTR*$^{+/+}$ *INK4a*$^{-/-}$ and G5 *mTR*$^{-/-}$ *INK4a*$^{-/-}$ ($p = 0.0052$) or G4 + G5 *mTR*$^{-/-}$ *INK4a*$^{-/-}$ ($p = 0.0072$) groups. The decreased tumors and increased survival in G4 and G5 *mTR*$^{-/-}$ *INK4a*$^{-/-}$ mice suggest that the significant telomere shortening and loss of telomere function in late-generation *mTR*$^{-/-}$ animals reduces cancer incidence in vivo in mice homozygous for the *INK4a*$^{\Delta 2/3}$ allele.

Impaired Cellular Growth and Colony Formation in Late-Generation *mTR*$^{-/-}$ *INK4a*$^{-/-}$ MEF Cultures

The reduction in tumorigenesis in the G4-G5 *INK4a*$^{-/-}$ mice could relate to an intrinsic growth defect in the developing cancer cell or to an inability of the host to provide a supportive environment for tumor formation. With respect to the latter, the host capacity required for tumorigenesis often necessitates robust proliferative responses (such as angiogenesis); it is therefore possible that the loss of telomere function in surrounding support cells could underlie the impaired tumorigenesis in the G4-G5 *INK4a*$^{-/-}$ mice. Thus, to compare more directly the intrinsic growth and tumorigenic potential of G5 *INK4a*$^{-/-}$ derived cells, primary mouse embryonic fibroblasts (MEFs) were isolated and analyzed in culture for colony formation and for susceptibility to transformation by cellular oncogenes.

Colony formation following low-density seeding has been used as a quantitative assay to measure the capacity of single cells to proliferate beyond senescence checkpoints and hence serves as an indicator of proliferative and immortalization potential (Kraemer et al., 1986; Conzen and Cole, 1995; Serrano et al., 1996). We have shown previously that *INK4a*$^{-/-}$ MEFs exhibit a greater than 200-fold increase in the rate of colony formation relative to *INK4a*$^{+/+}$ controls (Serrano et al., 1996). This high rate of colony formation affords an opportunity to uncover a potential negative impact of telomere shortening on proliferation and immortalization. In multiple independently derived cultures, G5 *mTR*$^{-/-}$ *INK4a*$^{-/-}$ MEFs showed a greatly reduced ability to form colonies (Figures 3A and 3B). The sole exception was one subclone, G5.7 *mTR*$^{-/-}$ *INK4a*$^{-/-}$, that produced a similar number of colonies as *mTR*$^{+/+}$ *INK4a*$^{-/-}$ controls (Figure 3A); however, these colonies were less dense and appeared senescent upon microscopic inspection (data not shown). Together, these results indicate that, while the absence of telomerase per se has no direct effect on the *INK4a*$^{-/-}$ phenotype, short dysfunctional telomeres are associated with a severe defect in growth and inability to escape senescence/crisis (see below).

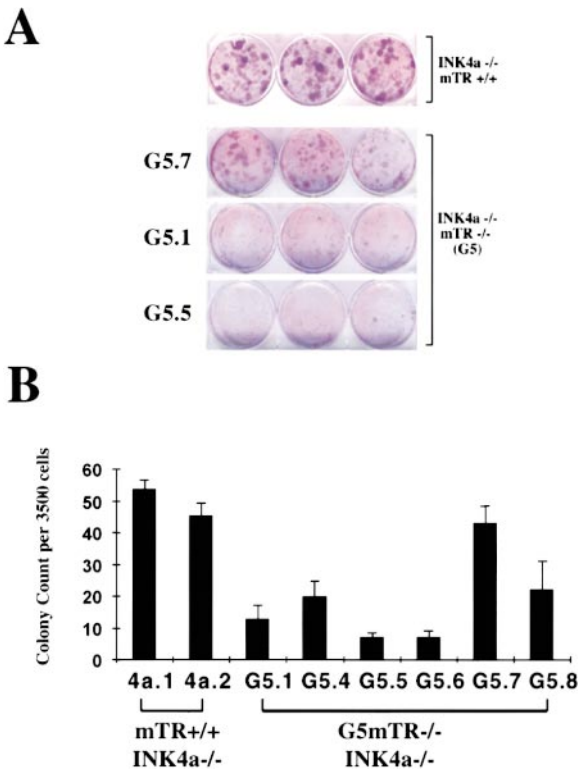

Figure 3. Decreased Colony Formation in G5 *mTR*$^{-/-}$ *INK4a*$^{-/-}$ MEFs

(A) Colony formation assay revealing diminished ability of G5 *mTR*$^{-/-}$ *INK4a*$^{-/-}$ MEFs to form detectable colonies following seeding at 3500 cells per 6 well plate and 8 days in culture. Note the diminished intensity of the colonies that appear for G5 *mTR*$^{-/-}$ samples (bottom three panels) in comparison to *mTR*$^{+/+}$ samples (top panel).

(B) Graphic illustration of the mean number of colonies appearing for each MEF culture per 6-well plate. Each bar represents the mean of three independent experiments.

Oncogenic Resistance of Late-Generation *mTR*$^{-/-}$ *INK4a*$^{-/-}$ Cells

Focus formation following c-Myc and H-*RAS*^{G12V} cotransfection provides a quantitative measurement of transformation potential. Previous studies have established that *INK4a*$^{-/-}$ MEFs generate a high number of Myc/RAS-induced transformed foci and that Myc/RAS oncogenic activity can be modulated by addition of genetic modifiers to the cotransfection (e.g., Pomerantz et al., 1998). As anticipated, several independent cotransfections demonstrated an equivalent number of Myc/RAS-induced foci in the *mTR*$^{+/+}$ *INK4a*$^{-/-}$ and G1-G2 *mTR*$^{-/-}$ *INK4a*$^{-/-}$ cultures (Figure 4A, G1 *mTR*$^{-/-}$ *INK4a*$^{-/-}$ not shown). In contrast, all independently derived G5 *mTR*$^{-/-}$ *INK4a*$^{-/-}$ cultures exhibited 1.5- to 40-fold reductions in the number of Myc/RAS foci relative to mTR $^{+/+}$ INK4a$^{-/-}$ controls (Figures 4A and 4B). Foci derived from the G5 *mTR*$^{-/-}$ *INK4a*$^{-/-}$ MEFs typically appeared 1 day later on average and were often smaller in size than those derived from *mTR*$^{+/+}$ *INK4a*$^{-/-}$ cells. The observed reductions in the rate of Myc/RAS focus formation for

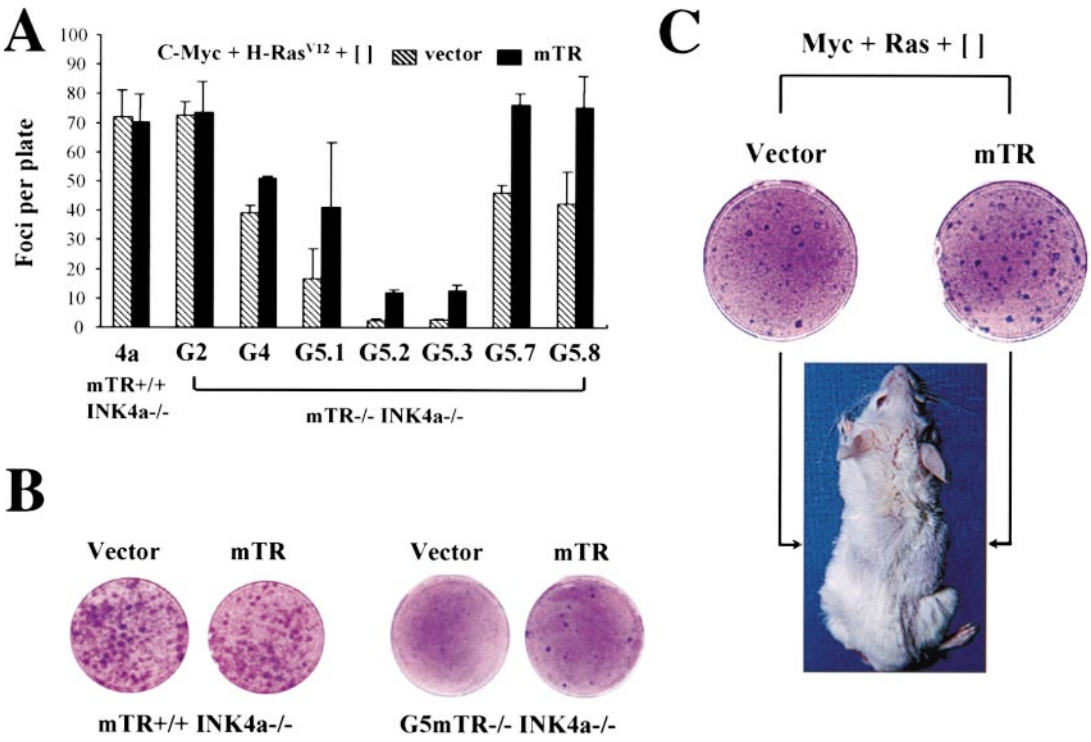

Figure 4. mTR Partially Rescues Myc/RAS Transformation of G5 *mTR*$^{-/-}$ *INK4a*$^{-/-}$ MEFs

(A) Graphic illustration of the number of foci per 10 cm plate 9 days following transfection of oncogenes Myc + RAS and either empty vector (hatched) or mTR (black).

(B) Representative plates of the same MEF culture transfected with Myc + RAS + empty vector or mTR. Plates were stained with 0.1% crystal violet.

(C) Growth of transformed cells in SCID mice. Entire plates transformed with Myc + RAS + vector (left) or mTR (right) were trypsinized and 5×10^5 cells were injected subcutaneously into SCID mice. Pictures were taken 12 days following injection.

late generations of *mTR*$^{-/-}$ *INK4a*$^{-/-}$ MEFs suggest that short telomeres attenuate the high transformation efficiency of INK4a deficiency.

mTR Rescue of Impaired Oncogenesis

To assess whether impaired oncogenic potential related to the loss of telomere function, a genomic subclone encoding the *mTR* gene (or an empty vector) was added to the Myc/RAS cotransfections. This *mTR* fragment ("mTR") was shown to restore telomerase activity in *mTR*$^{-/-}$ MEFs (Blasco et al., 1997; Chin et al., 1999 [this issue of *Cell*]) and 5 of 5 Myc/RAS/mTR transformed subclones exhibited TRAP activity (data not shown). Compared to vector, the addition of mTR to Myc/RAS cotransfections produced no increase in foci counts in wild-type and G2 *mTR*$^{-/-}$ *INK4a*$^{-/-}$ MEFs and only modest increases in G4 *mTR*$^{-/-}$ *INK4a*$^{-/-}$ MEFs (Figure 4A). In contrast, mTR cotransfection resulted in a 2- to 5.5-fold increase in the rate of Myc/RAS-induced foci in the G5 *mTR*$^{-/-}$ *INK4a*$^{-/-}$ MEFs (Figures 4A and 4B). Additionally, mTR transfection enhanced the subcloning efficiency of G5 Myc/RAS (i.e., the capacity of foci to yield permanently established cell lines). The subcloning efficiencies were 5 of 20 (25%) for Myc/RAS/vector ("vector") cotransfections versus 13 of 21 (62%) for Myc/RAS/mTR ("mTR") cotransfections ($p = 0.008$).

To understand further the role of mTR in oncogenic transformation of *mTR*$^{-/-}$ *INK4a*$^{-/-}$ MEFs, the latency of tumor formation in vivo was examined in tumor transplantation assays. Cells (1×10^6) were harvested from a plate containing foci generated from cultures cotransfected with Myc/RAS and mTR or empty vector (vector). These cells were injected into SCID mice to assess the rates of tumor formation. Dramatic differences in tumor latency were observed (Figure 4C). The mTR cultures produced visible tumors in 4 to 7 days following injection and grew to approximately 2 cm after 14 days, while the vector cultures failed to produce tumors during the same period. However, it is notable that the vector cultures did eventually yield tumors and, once established, these tumors were equally aggressive and histologically indistinguishable from the mTR expressing tumors (data not shown). The rescue of oncogenic transformation and restoration of telomerase by mTR transfection suggest that the compromised growth properties of G5 *mTR*$^{-/-}$ *INK4a*$^{-/-}$ MEFs result primarily from a loss of telomere function. By extension, these findings also suggest that the reduced tumor incidence in late-generation *mTR*$^{-/-}$ INK4a$^{-/-}$ mice relates in large part to a cell-autonomous defect due to loss of telomere function in the developing cancer cell.

Telomere Dynamics and Cytogenetic Profiles in the Setting of Telomere Dysfunction and Tumorigenesis

The ability of late-generation *mTR*$^{-/-}$ *INK4a*$^{-/-}$ cells to form tumors after extended growth periods (Figure 4C

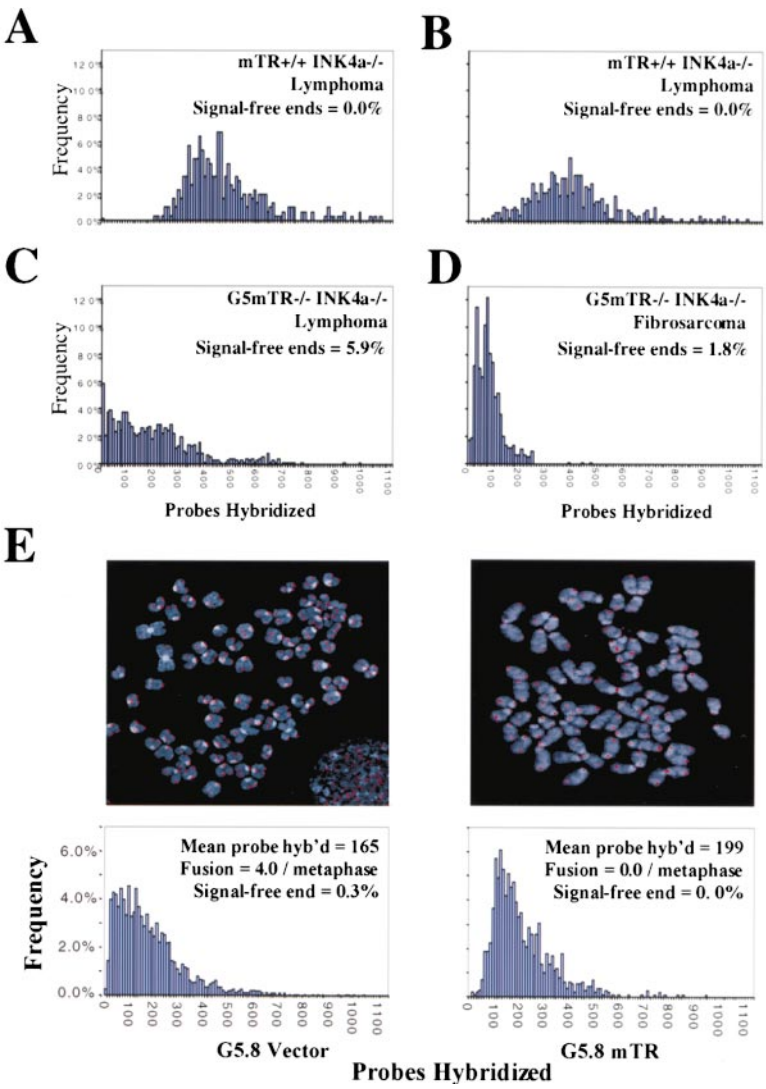

Figure 5. Telomere Dynamics in Telomerase Positive and Negative Tumors

(A–D) Histogram profiles of the number of probes hybridized for two $mTR^{+/+}$ $INK4a^{-/-}$ and two G5 $mTR^{-/-}$ $INK4a^{-/-}$ tumors as indicated. The frequency of 0 probes hybridized represents the percentage of free chromosomal termini lacking detectable telomeric signal and does not include missing repeats at chromosome fusion points.

(E) Metaphase spreads (top two panels) of SCID tumors derived from Myc/RAS transformed G5 $mTR^{-/-}$ $INK4a^{-/-}$ MEF (G5.8) with or without telomerase reconstitution ("mTR" or "vector", respectively). Separate chromosome DAPI and cy3 telomere images were overlaid in Adobe Photoshop (Adobe Systems, Mountain View, California) and assigned blue and red colors, respectively. (Bottom panels) telomere length histograms represented by the number of probes hybridized per telomere.

and see Blasco et al., 1997) suggests the existence of telomerase-independent telomere maintenance mechanisms or neutralization of cellular checkpoints elicited by telomere erosion. To begin to assess these adaptive responses, quantitative telomere length determinations and cytogenetic analyses were conducted on $mTR^{-/-}$ $INK4a^{-/-}$ cell lines and tumors.

Primary Tumors

First, telomere length and cytogenetic analyses were performed in primary tumors arising in G5 $mTR^{-/-}$ $INK4a^{-/-}$ and $mTR^{+/+}$ $INK4a^{-/-}$ mice. Telomere length was measured by quantitative fluorescence in situ hybridization (Q-FISH) (Zijlmans et al., 1997). As anticipated, the G5 $mTR^{-/-}$ $INK4a^{-/-}$ tumors possessed a shorter mean telomere length than the $mTR^{+/+}$ $INK4a^{-/-}$ tumors (Figures 5A–5D). These primary G5 $mTR^{-/-}$ $INK4a^{-/-}$ tumors showed chromosomal termini lacking detectable hybridization signal (termed "signal-free ends"). For example, a G5 $mTR^{-/-}$ $INK4a^{-/-}$ lymphoma possessed 5.9% signal-free ends and 1 fusion per metaphase, and a G5 $mTR^{-/-}$ $INK4a^{-/-}$ fibrosarcoma had 1.8% signal-free ends (Figures 5C and 5D) and 1 fusion per metaphase. In contrast, metaphases derived from a collection of $mTR^{+/+}$ $INK4a^{-/-}$ lymphomas and fibrosarcomas revealed 0.1% signal-free ends per metaphase (n = 40) (Figures 5A and 5B) and 0.03 fusions per metaphase. These data indicate that primary tumor formation in vivo can take place in the setting of severely shortened telomeres and telomere dysfunction (i.e., fusions).

Culture-Derived Tumors in SCID Mice

Decreased tumor incidence and focus formation in the setting of compromised telomere function (see above) implies the existence of a genetic selection process that enables late-generation *mTR* null cancer cells to survive despite telomere dysfunction. Such genetic adaptations may not be readily evident in the analysis of a limited pool of primary tumors (see above) or independently derived Myc/RAS transformed cell lines (see below). To study the most malignant subclones, we allowed selection for these cells to occur in vivo by generating tumors in SCID mice produced from the injection of Myc/RAS transformed MEF cultures (e.g., SCID tumors in Figure 4C). Both telomere length and cytogenetic profiles in the

Table 1. Summary of Telomere Length and Cytogenetic Profiles in G5 *mTR*$^{-/-}$ *INK4a*$^{-/-}$ Transformed Subclones

	Mean Probes per Telomere	Fusion per Metaphase	No. of Metaphases Examined
G5.7 parental	323	0.6	15
7.1 vector	72	2.8	10
7.2 vector	33	2.8	10
7.3 vector	35	3.0	10
7.4 mTR	70	0.2	10
7.5 mTR	36	0.1	10
7.6 mTR	435	0.2	10

Metaphase spreads were prepared as described in Experimental Procedures, and fusions per metaphase were counted. Probes per telomere were determined by Q-FISH as described in Experimental Procedures.

parental G5 *mTR*$^{-/-}$ *INK4a*$^{-/-}$ MEF cultures and tumors produced from these MEF cultures cotransfected with either Myc/RAS/vector or Myc/RAS/mTR were analyzed. A representative metaphase for each of the "culture-derived" tumors is shown (Figure 5E). Tumors derived from both the vector and mTR cotransformed cells showed a striking reduction in the number of signal-free chromosome termini ($< 0.3\%$ or 0.0%, respectively, $n = 15$ metaphases for each) compared with the 1.7% signal-free ends in the parental culture ($n = 15$) (data not shown). Remarkably, despite this similar decrease in the number of signal-free ends, the vector-derived transformants possessed 4 fusions per metaphase ($n = 15$), whereas no fusion was observed for mTR transformants ($n = 15$) (Figure 5E, top left and right panels, respectively). This is compared to an average of 0.6 fusion per metaphase observed for the G5.8 parental cultures ($n = 15$) (data not shown). Thus, in cells with short telomeres, tumor growth appears to select for an increase in the number of chromosomal fusions and a decrease in the occurrence of signal-free ends. Together, these findings suggest that viability in vector-derived tumors may be enhanced through chromosomal fusions, and/or reduction of DNA damage signals (i.e., decreased signal-free ends).

Myc/RAS Transformed Subclones

To further analyze the changes in telomere length and chromosome fusions between telomerase negative and telomerase positive transformed cells, we performed similar analyses on independently derived transformed cell lines arising from a G5 *mTR*$^{-/-}$ *INK4a*$^{-/-}$ MEF culture, G5.7. Q-FISH analysis of three Myc/RAS/mTR and three Myc/RAS/Vector derived cell lines revealed that all vector metaphases possessed shorter telomeres relative to those derived from the parental G5.7 culture (Table 1). Telomere lengths also decreased in 2 of 3 mTR subclones (7.4 and 7.5, Table 1) but increased in the remaining subclone (7.6). Interestingly, subclone 7.6 showed long heterogeneous telomeres, reminiscent of ALT pathway cells, despite possessing telomerase activity. Chromosomal end fusions were detected in all vector metaphases, with an average of 2.9 fusions per metaphase ($n = 30$). Conversely, fusions were rare in the mTR metaphases with an average of only 0.1 fusions per metaphase ($n = 30$). Notably, although mTR subclones 7.4 and 7.5 possessed a similar or shorter overall telomere length relative to the vector subclone 7.1, both 7.4 and 7.5 mTR clones exhibited far fewer fusions than the 7.1 vector sample (Table 1). These findings, in combination with the cytogenetic analysis of SCID-derived tumors (Figure 5E), suggest that the presence of telomerase in tumor cells can stabilize telomeres at shorter lengths and provide genomic stability possibly via a protective "capping function."

Finally, we analyzed the ability of the mTR and vector transfected subclones to form tumors in SCID mice. All three vector transfected subclones exhibited tumor growth characteristics that were identical to the mTR transfected subclones despite the presence of shorter telomeres and multiple fusions. For both vector and mTR transformed cells, the subcutaneous injection of 5×10^5 cells into SCID mice produced 2 cm tumors in 10 to 14 days (data not shown). In addition, the vector transfected subclone 7.3 grew at a rate similar to the mTR transfected subclone 7.6 through four cycles of repeated injection into SCID mice (Data not shown).

Rescue of Impaired Oncogenesis by SV40 Large T Antigen

Given the striking difference in cytogenetic profile between Myc + RAS transformed MEFs containing either mTR or a vector control plasmid, we speculate that mTR may be enhancing focus formation by diminishing the rampant genetic instability associated with telomere dysfunction. Recent evidence has directly implicated the p53-dependent DNA damage response as a key mediator of the adverse cellular consequences (e.g., apoptosis) brought about by telomere dysfunction (Chin et al., 1999; Karlseder et al., 1999). Abrogation of these responses through the use of a viral oncoprotein such as SV40 large T antigen (T-Ag) would therefore be predicted to produce similar numbers of transformed foci in late-generation *mTR*$^{-/-}$ *INK4a*$^{-/-}$ MEFs transfected with either mTR or vector control plasmids. To this end, we performed transformation assays on G5 *mTR*$^{-/-}$ *INK4a*$^{-/-}$ MEFs by cotransfecting T-Ag + RAS with either vector control or mTR (Figure 6). Total number of foci for three different G5 *mTR*$^{-/-}$ *INK4a*$^{-/-}$ MEF cultures were only modestly reduced compared to the *mTR*$^{+/+}$ *INK4a*$^{-/-}$ MEF cultures (Figure 6A). More importantly, mTR did not significantly enhance numbers of foci for any of the three G5 *mTR*$^{-/-}$ *INK4a*$^{-/-}$ above that of vector control groups. The ability of T-Ag to transform these late-generation *mTR*$^{-/-}$ *INK4a*$^{-/-}$ MEFs with or without telomerase reconstitution with equal efficiency suggests that T-Ag may be capable of neutralizing cellular checkpoints downstream of telomere dysfunction.

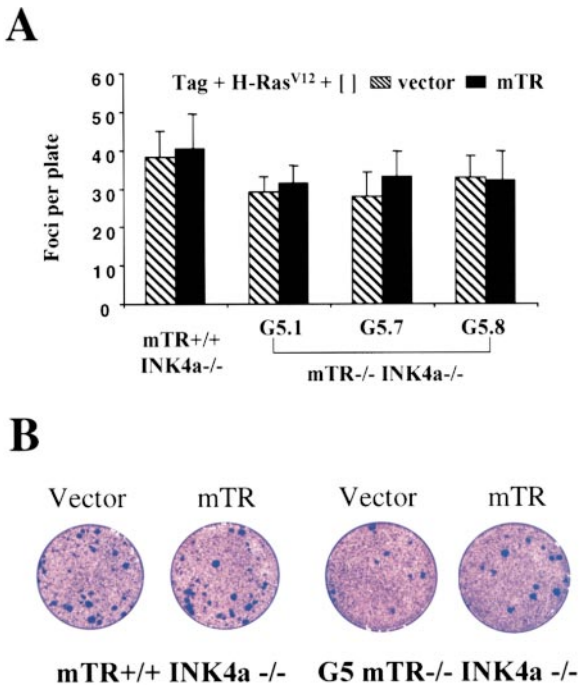

Figure 6. T-Ag Partially Rescues the Ability of G5 *mTR*$^{-/-}$ *INK4a*$^{-/-}$ MEFs to Form Transformed Foci

(A) Graphic illustration of number of foci per 10 cm plate 10 days after transfection of SV40 large T antigen (T-Ag) + RAS + either empty vector (hatched) or mTR (black). MEF cultures were split 1:3 18 hr after transfection.

(B) Representative plates of the same MEF culture transfected with T-Ag + RAS + empty vector or mTR as indicated. Plates were stained with 0.1% crystal violet for graphic illustration.

Indeed, with complete elimination of p53 function, telomere dysfunction can in fact increase the number of Myc/RAS-induced foci (Chin et al., 1999).

Discussion

Telomere maintenance via telomerase reactivation or ALT is a hallmark of cancer cells (Counter et al., 1992; Kim et al., 1994; Bryan et al., 1995, 1997). Here, the experimental merits of the INK4a$^{\Delta 2/3}$ model were exploited to study the role of telomerase in transformation and tumorigenesis. The loss of telomere function and the inability to activate telomerase reduced the cancer incidence by greater that 50% in vivo and enhanced survival. Notably the reduction in tumor formation was seen only in late generations after significant telomere shortening had occurred. Further, cell culture experiments using cells from late-generation animals demonstrated impaired colony formation, transformation, and plating efficiencies. Cytogenetic analysis indicated that these cells had loss of telomere function. The reintroduction of mTR greatly ameliorated the antioncogenic effects associated with telomere loss. Together, these findings establish an important role for intact telomeres and telomerase in facilitating the tumorigenic process.

This study also establishes that the response to telomere loss during cellular transformation is complex. In telomerase-deficient cells, we observed that long-term tumorigenic growth in the setting of short telomeres can be associated with an increase in dicentric chromosomes (and corresponding reduction in signal-free ends). Following very stringent tumorigenic selection (for example, Figure 5), there appears to be a marked decrease in the frequency of signal-free termini and a further increase in fusions. This suggests that end-to-end fusion represents in some cases an adaptive mechanism which serves to eliminate unprotected chromosomal termini and thereby maintains chromosomal integrity. The formation of chromosomal fusions in the G5 *mTR*$^{-/-}$ *INK4a*$^{-/-}$ derived primary tumor cells may represent a similar compensatory mechanism. Only in those cases where the fusion results in a stable Robertsonian type chromosome is this mechanism likely to be adaptive. Thus, such a mechanism may be more prevalent in mouse cells than human cells, since mouse chomosomes are telocentric (Kipling et al., 1991).

The tight correlation between telomere maintenance and human cancer has led to the proposed use of telomerase inhibition for the treatment of malignancy. We have demonstrated that when cells have significantly shortened telomeres, telomerase can cooperate with c-Myc and RAS to transform cells and generate tumors. It was shown recently that hTERT can cooperate with loss of tumor suppressor function and T-Ag to bypass M1 and M2 checkpoints, respectively (Counter et al., 1998; Kiyono et al., 1998). Thus, telomerase can function to enhance cellular transformation by oncogenes and in principle could provide a rational chemotherapeutic target for inhibition. In established tumors, however, telomerase inhibition may lead to crisis, but adaptive mechanisms such as fusion and/or ALT may give rise to survivor cells. Given the large telomeric reserve present in the mouse genome, it is difficult to achieve a state of global telomere shortening analogous to crisis in human cells. However, analysis of vector transformed subclones and primary G5 *mTR*$^{-/-}$ *INK4a*$^{-/-}$ tumor cells indicates that transformed cells can tolerate relatively high numbers of missing or very short telomeric repeats and chromosomal fusions that are characteristic of postcrisis human cells (Counter et al., 1992). The ability of SV40 large T antigen to transform late-generation *mTR*$^{-/-}$ *INK4a*$^{-/-}$ cells with near similar efficiency to *mTR*$^{+/+}$ *INK4a*$^{-/-}$ counterparts suggests that T-Ag may deactivate checkpoints which allow for tolerance of dysfunctional telomeres (Chin et al., 1999). Along these lines, the response to telomere-induced crisis may be very different in cancer cells harboring intact (INK4a/ARF) or compromised (p53) DNA damage pathways. Since DNA damage, such as telomere erosion, does not utilize ARF to signal to p53 (Kamijo et al., 1997; Stott et al., 1998), loss of telomeric function in an INK4a/ARF null tumor would be predicted to lead to apoptosis through a p53-dependent process. On the other hand, it is possible that the loss of telomere function combined with defective telomere sensing checkpoints (i.e., p53-dependent DNA damage response) may have either no effect or lead to an increase in genetic instability and enhanced malignant potential. Our recent studies suggest that the absence of telomerase does indeed fuel genetic instability and promote tumor formation in aging *mTR*$^{-/-}$ mice

(Rudolph et al., 1999). Thus, telomerase may play a paradoxical role, either promoting or inhibiting tumor formation depending on the genetic context. Further studies will be required to define the genetic backgrounds responsible for determining which role predominates. Our results point to the need for further investigation into the relationship between telomeres and key tumor suppressor pathways, particularly those involved in the response to DNA damage.

Experimental Procedures

Generation of mTR/INK4a Double Null Mice for Tumor Studies

Mice heterozygous at both the *INK4a* and *mTR* loci were obtained through crossing heterozygotes null for each individual locus to generate $mTR^{+/-}$ $INK4a^{+/-}$ animals in the predicted 1:4 ratio. Double heterozygotes produced doubly null mice again in the expected 1:16 ratio. These first-generation $mTR^{-/-}$ $INK4a^{-/-}$ (G1) were mated to give the second generation of telomerase deficiency (G2). This mating scheme was continued until the fifth generation (G5). This was the latest generation of telomerase-deficient $INK4a^{-/-}$ mice to be followed, as we were unable to obtain G6 animals due to infertility associated with late-generation *mTR* knockout mice. Tumor studies involving two-step carcinogenesis protocols were performed as previously described (Serrano et al., 1996).

Telomerase Assays

TRAP assays were performed with the TRAPezeTM kit (Oncor) as previously described (Greenberg et al., 1998). Assays were run on 1000 cells for fibrosarcoma cell lines from the $INK4a^{-/-}$ tumors, or from 1000 cells from tumor involved lymph nodes immediately after putting into single-cell suspension. Heat inactivation of each sample was performed at 85°C for 5 min prior to the primer elongation step.

Colony Formation

Cells were seeded in triplicate at 3500 cells per 6 well plate and kept in DMEM containing 15% FBS for 8 days. Following this period, cells were washed with PBS, fixed in methanol, and stained for 2–4 min with Giemsa stain. Colonies larger than 1 mm in diameter were counted.

Transformation Assays

MEF cultures at passage 2–5 were seeded at 5×10^5 cells per 10 cm plate 16 hr prior to transfection with 2 μg each of expression constructs for *myc* or T-Ag and H-RAS^{G12V} (Pomerantz et al., 1998), and either Bluescript KS(+) (Stratagene) vector control, or a genomic subclone of mTR (Blasco et al., 1997). Foci were counted 7 to 9 days after transfection. Plates were washed with PBS, fixed in methanol for 10 min, and then stained with either 0.1% crystal violet or giemsa for 2 min.

Tumor Growth in SCID Mice

Injection of transformed MEF cultures into SCID mice were performed by one of the following two methods. (1) MEF cultures transfected with either Myc/RAS/vector or Myc/RAS/mTR were trypsinized, and 1×10^6 cells were injected in both the posterior and anterior flank of two mice. Thus, one side contained two injection sites for vector transfected cells, and the opposing side contained two injection sites for the mTR transfected cells. (2) Individual foci were subcloned into 12-well plates from either the vector or mTR groups. Cells that maintained a transformed morphology were expanded into 10 cm plates and 5×10^5 cells were injected as described above. For both methods, mice were sacrificed when tumors reached 3 cm in diameter.

Quantitative FISH of Metaphase Chromosomes

Actively dividing cells were kept in 0.1 μM colcemid for 1–2 hr and then trypsinized to single-cell suspension. Cells were centrifuged at 1000 rpm for 10 min and supernatant removed by aspiration. The remaining cell pellet was resuspended in 0.075 M KCL warmed to 37°C and allowed to sit at room temperature for 10 min. The cells were centrifuged again and resuspended in 0.5 ml of the supernatant. Three milliliters of a 3:1 methanol:acetic acid fix solution was then added slowly with continuous bubbling to mix. The metaphase cells were then centrifuged and supernatant aspirated. Fix solution was again used to resuspend the pellet and the cells centrifuged. This step was repeated one more time. Cells were then dropped onto 22 mm by 22 mm glass coverslips (VWR) and allowed to air dry overnight.

Coverslips containing suitable metaphase chromosomes were hybridized to cy3-labeled peptide nucleic acid (PNA) probes $(C_3TA_2)_3$ and counterstained with DAPI as previously described (Zijlmans et al., 1997). Images were captured using CellScan software (Scanalytics, Fairfax, VA) on an Optiplex Gxpro computer (Dell, Austin, TX) with a CH-250 16-bit, thermoelectrically cooled (−40.0°C) charge coupled device (CCD) camera (Photometrics, Tuscon, AZ) mounted on a Provis AX70 fluorescence microscope (Olympus, Melville, NY). Twenty-five optical sections were captured at 100 μm z-intervals and at effective pixel size of 500 nm by 500 nm. Background was subtracted and the images exhaustively deconvoluted with an acquired point spread function (PSF) using EPR software (Scanalytics) (Bertrand et al., 1998).

The TFI per telomere was determined in the program MetamorphTM by circling cy3 intensities that corresponded to telomeric positions on the DAPI image of the chromosomes. The number of probes hybridized per telomere was determined by dividing the TFI of each telomere by the experimentally determined TFI per probe value and then by the number of planes restored in the PDF (Femino et al., 1998).

Acknowledgments

We thank members of the DePinho lab, particularly Ned Sharpless, for critical reading of the manuscript, Shailish Shenoy for expert advice on imaging and analysis of Q-FISH samples, and Lynn Emerson for outstanding administrative assistance. We are most grateful to the expert histological technical support from B. Furman, K. E. Cedeno-Baier, and L. Husted. This work was supported by grants from the National Institutes of Health (HD348880 and HD28317) and AHA grant-in-aid to R. A. D. NIH support to C. W. G. (CA16519) and to R. S. and A. F. (GM54887) is acknowledged. L. C. is supported by an NIH Mentored Clinician Scientist Award KO8AR02104. R. A. G. is supported by an NIH Training Grant 5T32GM07491. This work was done in partial fulfillment for the Ph.D. requirement for R. A. G.; R. A. D. is an American Cancer Society Research Professor. Support from the DFCI Cancer Core grant to R. A. D. and L. C. is acknowledged.

Received February 2, 1999; revised April 16, 1999.

References

Bacchetti, S. (1996). Telomere maintenance in tumor cells. Cancer Surv. *28*, 197–226.

Bates, S., Phillips, A.C., Clark, P.A., Stott, F., Peters, G., Ludwig, R.L., and Vousden, K.H. (1998). $p14^{ARF}$ links the tumor suppressors Rb and p53. Nature *395*, 124–125.

Bednarek, A.K., Chu, Y., Slaga, T.J., and Aldaz, C.M. (1997). Telomerase and cell proliferation in mouse skin papillomas. Mol. Carcinog. *20*, 329–331.

Bertrand, E., Chartrand, P., Schaefer, M., Shenoy, S.M., Singer, R.H., and Long, R.M. (1998). Localization of ASH1 mRNA particles in living yeast. Mol. Cell *2*, 437–445.

Blasco, M.A., Rizen, M., Greider, C.W., and Hanahan, D. (1996). Differential regulation of telomerase activity and telomerase RNA during multi-stage tumorigenesis. Nat. Genet. *12*, 200–204.

Blasco, M.A., Lee, H.W., Hande, M.P., Samper, E., Lansdorp, P.M., DePinho, R.A., and Greider, C.W. (1997). Telomere shortening and tumor formation by mouse cells lacking telomerase RNA. Cell *91*, 25–34.

Bodnar, A.G., Ouellette, M., Frolkis, M., Holt, S.E., Chiu, C.P., Morin, G.B., Harley, C.B., Shay, J.W., Lichsteiner, S., and Wright, W.E.

(1998). Extension of life-span by introduction of telomerase into normal human cells. Science *279*, 349–352.

Broccoli, D., Godley, L.A., Donehower, L.A., Varmus, H.E., and de-Lange, T. (1996). Telomerase activation in mouse mammary tumors: lack of detectable telomere shortening and evidence for regulation of telomerase RNA with cell proliferation. Mol. Cell. Biol. *16*, 3765–3772.

Bryan, T.M., Englezou, A., Gupta, J., Bacchetti, S., and Reddel, R.R. (1995). Telomere elongation in immortal human cells without detectable telomerase activity. EMBO *14*, 4240–4248.

Bryan, T.M., Marusic, L., Bacchetti, S., Namba, M., and Reddel, R.R. (1997). The telomere lengthening mechanism in telomerase-negative immortal human cells does not involve the telomerase RNA subunit. Hum. Mol. Genet. *6*, 921–926.

Chadeneau, C., Siegel, P., Harley, C.B., Muller, W.J., and Bacchetti, S. (1995). Telomerase activity in normal and malignant murine tissues. Oncogene *11*, 893–898.

Chin, L., Artandi, S.E., Shen, Q., Tam, A., Lee, S.-L., Gottlieb, G.J., Greider, C.W., and Depinho, R.A. (1999). p53 deficiency rescues the adverse effects of telomere loss and cooperates with telomere dysfunction to accelerate carcinogenesis. Cell *97*, this issue, 527–538.

Conzen, S.D., and Cole, C.N. (1995). The three transforming regions of SV40 T antigen are required for immortalization of primary mouse embryo fibroblasts. Oncogene *11*, 2295–2302.

Counter, C.M., Avilion, A.A., LeFeuvre, C.E., Stewart, N.G., Greider, C.W., Harley, C.B., and Bacchetti, S. (1992). Telomere shortening associated with chromosome instability is arrested in immortal cells which express telomerase activity. EMBO *11*, 1921–1929.

Counter, C.M., Hahn, W.C., Wei, W., Caddle, S.D., Beijersbergen, R.L., Lansdorp, P.M., Sedivy, J.M., and Weinberg, R.A. (1998). Dissociation among in vitro telomerase activity, telomere maintenance, and cellular immortalization. Proc. Natl. Acad. Sci. USA *95*, 14723–14728.

de Stanchina, E., McCurrach, M.E., Zindy, F., Shieh, S.-Y., Ferbeyre, G., Samuelson, A.V., Prives, C., Roussel, M.F., Sherr, C.J., and Lowe, S.W. (1998). E1A signaling to p53 involves the $p19^{ARF}$ tumor suppressor. Genes Dev. *12*, 2434–2442.

Dykhuizen, D. (1974). Evolution of cell senescence, atherosclerosis and benign tumors. Nature *251*, 616–618.

Femino, A.M., Fay, F.S., Fogarty, K., and Singer, R.H. (1998). Visualization of single RNA transcripts in situ. Science *280*, 585–590.

Greenberg, R.A., Allsopp, R.C., Chin, L., Morin, G.B., and DePinho, R.A. (1998). Expression of mouse telomerase reverse transcriptase during development, differentiation and proliferation. Oncogene *16*, 1723–1730.

Greenberg, R.A., O'Haga, R.C., Deng, H., Xiao, Q., Hann, S.R., Adams, R.R., Lichsteiner, S., Chin, L., Morin, G., and DePinho, R.A. (1999). Telomerase reverse transcriptase gene is a direct target of c-Myc but is not functionally equivalent in cellular transformation. Oncogene *18*, 1219–1226.

Hara, E., Tsurui, H., Shinozaki, A., Nakada, S., and Oda, K. (1991). Cooperative effect of antisense-Rb and antisense-p53 oligomers on the extension of life span in human diploid fibroblasts, TIG-1. Biochem. Biophys. Res. Comm. *179*, 528–534.

Harley, C.B., Futcher, A.B., and Greider, C.W. (1990). Telomeres shorten during ageing of human fibroblasts. Nature *345*, 458–460.

Hayflick, L., and Moorehead, P.S. (1961). The serial cultivation of human diploid strains. Exp. Cell. Res. *25*, 585–621.

Kamijo, T., Zindy, F., Roussel, M.F., Quelle, D.E., Downing, J.R., Ashmun, R.A., Grosveld, G., and Sherr, C.J. (1997). Tumor suppression at the mouse *INK4a* locus mediated by the alternative reading frame product $p19^{ARF}$. Cell *91*, 649–659.

Kamijo, T., Weber, J.D., Zambetti, G., Zindy, F., Roussel, M.F., and Sherr, C.J. (1998). Functional and physical interactions of the ARF tumor suppressor with p53 and Mdm2. Proc. Natl. Acad. Sci. USA *95*, 8292–8297.

Karlseder, J., Broccoli, D., Dai, Y., Hardy, S., and deLange, T. (1999). P53- and ATM-dependent apoptosis induced by telomeres lacking TRF2. Science *283*, 1321–1325.

Kim, N.W., Piatyszek, M.A., Prowse, K.R., Harley, C.B., West, M.D., Ho, P.L., Coviello, G.M., Wright, W.E., Weinrich, S.L., and Shay, J.W. (1994). Specific association of human telomerase activity with immortal cells and cancer. Science *266*, 2011–2015.

Kipling, D., Ackford, H.E., Taylor, T.A., and Cooke, H.J. (1991). Mouse minor satellite genetically maps to the centromere and is physically linked to the proximal telomere. Genomics *11*, 235–241.

Kiyono, T., Foster, S.A., Koop, J.I., McDougall, J.K., Galloway, D.A., and Klingelhutz, A.J. (1998). Both $Rb/p16^{INK4a}$ inactivation and telomerase activity are required to immortalize human epithelial cells. Nature *396*, 84–88.

Kraemer, P.M., Ray, F.A., Brothman, A.R., Bartholdi, M.F., and Cram, L.S. (1986). Spontaneous immortalization rate of cultured Chinese hamster cells. J. Natl. Cancer Inst. *76*, 703–709.

Lee, H.W., Blasco, M.A., Gottlieb, G.J., Horner, J.W., Greider, C.W., and DePinho, R.A. (1998). Essential role of mouse telomerase in highly proliferative organs. Nature *392*, 569–574.

Lin, A.W., Barradas, M., Stone, J.C., van Aelst, L., Serrano, M., and Lowe, S. (1998). Premature senescence involving p53 and p16 is activated in response to constituitive MEK/MAPK mitogenic signaling. Genes Dev. *12*, 3008–3019.

Lloyd, A.C, Obermuller, F., Staddon, S., Barth, C.F., McMahon, M., and Land, H. (1997). Cooperating oncogenes converge to regulate cyclin/cdk complexes. Genes Dev. *11*, 663–677.

Lundblad, V., and Blackburn, E.H. (1993). An alternative pathway for yeast telomere maintenance rescues est1- senescence. Cell *73*, 347–360.

Martin-Rivera, L., Herrera, E., Albar, J.P., and Blasco, M.A. (1998). Expression of mouse telomerase catalytic subunit in embryos and adult tissues. Proc. Natl. Acad. Sci. USA *95*, 10471–10476.

McEachern, M.J., and Blackburn, E.H. (1996). Cap-prevented recombination between terminal telomeric repeat arrays (telomere CPR) maintains telomeres in Kluyveromyces lactis lacking telomerase. Genes Dev. *10*, 1822–1834.

Naito, T., Matsuura, A., and Ishikawa, F. (1998). Circular chromosome formation in a fission yeast mutant defective in two ATM homologues. Nat. Genet. *20*, 203–206.

Nakamura, T.M., Cooper, J.P., and Cech, T.R. (1998). Two modes of survival of fission yeast without telomerase. Science *282*, 493–496.

Niida, H., Matsumoto, T., Satoh, H., Shiwa, M., Tokutake, Y., Furuichi, Y., and Shinkai, Y. (1998). Severe growth defect in mouse cells lacking the telomerase RNA component. Nat. Genet. *19*, 203–206.

Palermo, I., Pantoja, C., and Serrano, M. (1998). $p19^{ARF}$ links the tumor suppressor p53 to Ras. Nature *395*, 125–126.

Pomerantz, J., Schreiber-Agus, N., Liegeois, N.J., Silverman, A., Alland, L., Chin, L., Potes, J., Orlow, I., Lee, H.W., Cordon-Cardo, C., and DePinho, R.A. (1998). The *INK4a* tumor suppressor gene product, $p19^{ARF}$, interacts with MDM2 and neutralizes MDM2's inhibition of p53. Cell *92*, 713–723.

Prowse, K.R., and Greider, C.W. (1995). Developmental and tissue-specific regulation of mouse telomerase and telomere length. Proc. Natl. Acad. Sci. USA *92*, 4818–4822.

Radfar, A., Unnikrishnan, I., Lee, H.W., DePinho, R.A., and Rosenberg, N. (1998). p19(Arf) induces p-53-dependent apoptosis during abelson virus-medicated pre-B cell transformation. Proc. Natl. Acad. Sci. USA *95*, 13194–13199.

Rudolph, K.L., Chang, S., Lee, H-W., Blasco, M., Gottlieb, G.J., Greider, C., and DePinho, R.A. (1999). Longevity, stress response, and cancer in aging telomerase deficient mice. Cell. *96*, 701–712.

Sager, R. (1991). Senescence as a mode of tumor suppression. Environ. Health Perspect. *93*, 59–62.

Serrano, M., Hannon, G.J., and Beach, D. (1993). A new regulatory motif in cell cycle control causing specific inhibition of cyclin D/cdk4. Nature *366*, 704–707.

Serrano, M., Lee, H., Chin, L., Cordon-Cardo, C., Beach, D., and DePinho, R.A. (1996). Role of the INK4a locus in tumor suppression and cell mortality. Cell *85*, 27–37.

Shay, J.W., Pereira-Smith, O., and Wright, W.E. (1991). A role for both RB and p53 in the regulation of human cellular senescence. Exp. Cell Res. *196*, 33–39.

Sherr, C.J. (1998). Tumor surveillance via the ARF-p53 pathway. Genes Dev. *12*, 2984–2991.

Stott, F.J., Bates, S., James, M.C., McConnell, B.B., Starborg, M., Brookes, S., Palmero, I., Ryan, K., Hara, E., Vousden, K.H., and Peters, G. (1998). The alternative product from the human CDKN2A locus, p14(ARF), participates in a regulatory feedback loop with p53 and MDM2. EMBO J. *17*, 5001–5014.

Vaziri, H., and Benchimol, S. (1998). Reconstitution of telomerase activity in normal human cells leads to elongation of telomeres and extended replicative life span. Curr. Biol. *8*, 279–282.

Wang, J., Xie, L.Y., Allan, S., Beach, D., and Hannon, G.J. (1998). Myc activates telomerase. Genes Dev. *12*, 1769–1774.

Wright, W.E., and Shay, J.W. (1995). Time, telomeres and tumours: is cellular senescence more than an anticancer mechanisms? Trends Cell Biol. *5*, 293–297.

Wu, K.J., Grandori, C., Amacker, M., Simon-Vermot, N., Polack, A., Lingner, J., and Dalla-Favera, R. (1999). Direct activation of TERT transcription by c-Myc. Nat. Genet. *21*, 220–224.

Zhang, Y., Xiong, Y., and Yarbrough, W.G. (1998). ARF promotes MDM2 degradation and stabilizes p53: *ARF-INK4a* locus deletion impairs both the Rb and p53 tumor suppressor pathways. Cell *92*, 725–734.

Zhu, J., Woods, D., McMahon, M., Bishop, J.M. (1998). Senescence of human fibroblasts induced by oncogenic Raf. Genes Dev. *12*, 2997–3007.

Zijlmans, J.M., Martens, U.M., Poon, S.S., Raap, A.K., Tanke, H.J., Ward, R.K., and Lansdorp, P.M. (1997). Telomeres in the mouse have large inter-chromosomal variations in the number of T2AG3 repeats. Proc. Natl. Acad. Sci. USA *94*, 7423–7428.

Zindy, F., Eischen, C.M., Randle, D.H., Kamijo, T., Cleveland, J.L., Sherr, C.J., and Roussel, M.F. (1998). Myc signaling via the ARF tumor suppressor regulates p53-dependent apoptosis and immortalization. Genes Dev. *12*, 2424–2433.